

Monolithically integrated twin ring diode lasers with quantum-dot active region

Hongjun Cao^a, Allen L. Gray^b, Luke F. Lester^a, Marek Osinski^{*a}

^a Center for High Technology Materials, University of New Mexico, 1313 Goddard SE, Albuquerque, New Mexico 87106-4343

^b Zia Laser, Inc., 801 University Blvd. SE, Suite 105, Albuquerque, New Mexico 87106

ABSTRACT

Optoelectronic integrated circuits incorporating twin ring diode lasers with InAs/InGaAs/GaAs quantum-dot active region have been fabricated and characterized. Directional control and unidirectional operation of ring diode lasers are demonstrated by forward biasing an S-section waveguide incorporated within the ring cavity. Mode-beating spectra from individual ring diode lasers are observed at three bands near 7.5 GHz, 16.6 GHz, and 25.1 GHz, corresponding to single, double, and triple longitudinal mode spacing in the ring cavity. In addition, mode beating spectra between optically independent integrated twin ring diode lasers are also demonstrated, with minimal linewidth of ~ 4 MHz.

Keywords: Diode laser, ring laser, quantum dot laser, optoelectronic integrated circuits

1. INTRODUCTION

Ring diode lasers are attractive as light sources for monolithic integration in optoelectronic integrated circuits (OEICs) because neither cleaved facets nor gratings are required for optical feedback. Their possible applications include mode-locking, ultrashort pulse generation, and switching. They are also of interest in optical inertial rotation sensors utilizing the Sagnac effect [1], in which the beat frequency shift between two counterpropagating lasing beams is directly proportional to the applied angular velocity. For this application, large-size rings are desirable in order to enhance the Sagnac frequency shift. Quantum-dot (QD)-based active regions are a natural choice for large-size ring diode lasers, because of demonstrated low threshold current densities and low internal losses in edge-emitting lasers [2]. In this paper, we report on fabrication and characterization of OEICs featuring twin ring diode lasers based on InAs/InGaAs/GaAs quantum-dot active region. Each ring cavity is integrated with an S-section for the purpose of directional control and unidirectional operation. Mode-beating spectra from individual ring diode lasers are measured at three bands, corresponding to single, double, and triple longitudinal mode spacing in the ring cavity. Finally, mode beating between optically independent twin ring diode lasers is also demonstrated.

2. OEIC DEVICE FABRICATION

The ring laser-based OEIC is fabricated using an MBE-grown 6-stack InAs/InGaAs/GaAs “dots-in-a-well” (DWELL) QD structure [2]. InAs QDs are embedded inside 5-nm-thick strained $\text{In}_{0.15}\text{Ga}_{0.85}\text{As}$ quantum wells (QWs) with 15-nm-thick GaAs barriers. The total thickness of the QD active region is ~ 135 nm. Details of the epitaxial layers of the DWELL wafer structure are given in Fig. 1. The lasing wavelength in all fabricated ring lasers is ~ 1.24 μm , corresponding to the ground-state emission of QDs.

A topological view of the OEIC device is shown schematically in Fig. 2. The monolithically integrated OEIC comprises two ridge-waveguide ring lasers, four directional coupling waveguides, one Y-junction mixer, and seven photodetectors (PDs). The racetrack-shaped rings have 1-mm radius of curvature and 2-mm-long straight sections, with total cavity length of 10.28 mm. Each ring incorporates an S-section element to favor unidirectional operation [3, 4]. All the ridge-

* Contact author: osinski@chtm.unm.edu; Tel. (505) 272-7812; Fax (505) 272-7801

waveguide structures are 3- μm wide, designed for a single-transverse-and-lateral-mode transmission. The straight sections of ring lasers form parts of directional couplers with 3- μm -wide external waveguides that deliver the laser light to monitoring PDs and to a mixer section. The edge-to-edge distance between the waveguides in the coupler is 2 μm , which results in 1-3% evanescent outcoupling of the lasing light. The distance between the two waveguides before they are combined into a Y-junction mixer is 0.6 mm. The mixer can be used to combine the CCW wave from ring laser R1 and CW wave from ring laser R2 for frequency beating [5]. In order to minimize reflections at the waveguide-detector junctions, the integrated PDs are cut at a Brewster angle at the tapered ends of each outcoupling waveguide. The size of the PDs is (200 μm) \times (400 μm), excluding the additional area arising from the Brewster angle cut. A branched-off waveguide conducts portion of the mixed light to the chip edge at a tilted angle for direct optical output.

p^{++} -GaAs cap layer, 60 nm
p^{++} -Al _{0.66-0} Ga _{0.34-1} As, graded, 40 nm
p^{+} -Al _{0.66} Ga _{0.34} As, upper clad, 700 nm
p -Al _{0.66} Ga _{0.34} As, upper clad, 600 nm
Undoped Al _{0-0.66} Ga _{1-0.34} As, graded, 10 nm
6 InAs QD stacks, 7 GaAs barriers, 135 nm
Undoped Al _{0.66-0} Ga _{0.34-1} As, graded, 10 nm
n -Al _{0.66} Ga _{0.34} As, lower clad, 600 nm
n^{+} -Al _{0.66} Ga _{0.34} As, lower clad, 700 nm
n^{+} -Al _{0-0.66} Ga _{1-0.34} As, graded, 40 nm
n^{+} -GaAs buffer, 300 nm
n^{+} -GaAs substrate

Fig. 1. MBE-grown InAs/InGaAs/GaAs dots-in-a-well (DWELL) laser wafer structure. The active region is 135-nm thick and composed of 6-stack InAs QDs that are embedded inside 5-nm-thick strained InGaAs QWs with 15-nm-thick GaAs barriers.

In device fabrication, all the elements mentioned above are defined in a single photolithography step and formed by dry etching using inductively coupled plasma (ICP). In a second dry etching step, deep isolation trenches are formed along boundaries of ring lasers, waveguides, and photodetectors. These trenches cut across the active region in order to reduce possible electrical crosstalk. Next, the OEIC is planarized using BCB, and p -side contacts (Ti/Pt/Au and thicker bonding metallization Ti/Au) are deposited. The ring lasers, S-sections, couplers, mixer, and photodetectors all have separate and independent metal contacts. Integrated Ti/Pt/Au 20- μm -wide stripe Joule heaters with the resistance of $\sim 20 \Omega$, located along the inner sides of ring ridges and residing on top of BCB, are added for thermal tuning of lasing wavelength. We reported a similar OEIC structure before, but with quantum-well active region and with spiral outcouplers instead of the S-section elements [5].

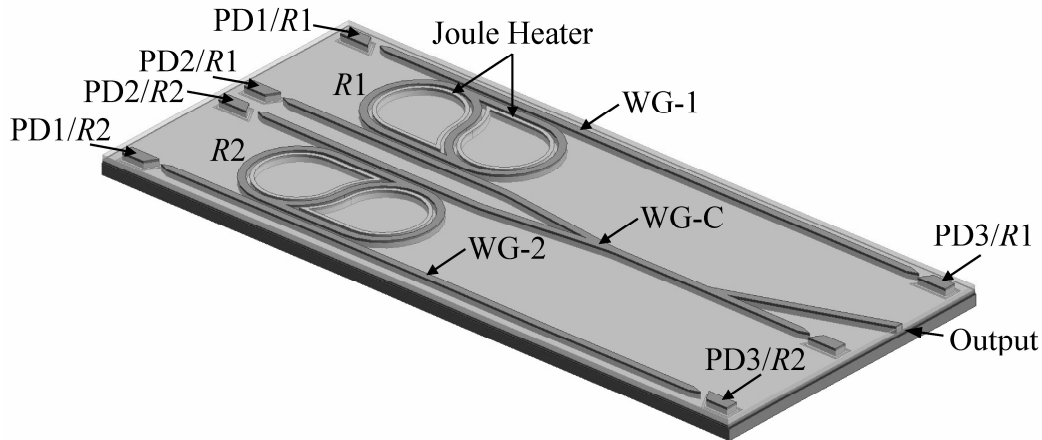


Fig. 2. Topological view of the OEIC structure, with exaggerated width and heights of integrated ridge-waveguide elements. The integrated ring diode lasers, S-section waveguides, coupling waveguides and mixer, and photodetectors all have separate and independent metal contacts.

3. ELECTRICAL AND OPTICAL CHARACTERIZATION

3.1 Current-voltage (I - V) characteristics

Current-voltage (I - V) and light-current (L - I) characteristics are measured for QD ring diode lasers R1 and R2 on the OEIC device. Fully packaged device is placed on a thermostabilized holder and a constant temperature is maintained during tests under dc current injection. A dual-channel Newport 8000 current source is used to pump the ring lasers and to drive the thermo-electric cooler (TEC) controller. Another Newport modular laser controller Model 8008 is used to drive the waveguide mixer WG-C. A 4832-C 4-channel power meter is used to detect the photocurrent output through integrated photodetectors, which measure the outcoupling from the directional circulating power in the rings. For the ring laser R2 as an example (see Fig. 2), the photocurrent signals taken simultaneously from the integrated photodiodes PD1/R2 and PD2/R2 correspond to the clockwise and counterclockwise traveling waves in the ring cavity, respectively. The ratio of these two signals is a measure of the ring laser unidirectionality and defined as counterpropagating wave suppression ratio (CWSR). These measurements are conducted in steps of 10 or 20 mA in the range from zero up to 1200 mA. The data are collected and processed by a computer running LabVIEW.

A typical I - V curve measured on ring laser R2 is shown in Fig. 3, indicating a normal p - n junction characteristic. We also tried to analyze the differential I - V curves, which have been investigated with QW-based ring lasers and proved to be useful for diagnostics of lasing threshold and directional power switching [6]. However, in the case of the QD-based ring lasers, no kinks were observed in their differential I - V curves at threshold. This could be due to their heterointerfaces not being sufficiently well graded during the epitaxial growth.

3.2 Highly unidirectional operation

In a ring diode laser, if both loss and gain are symmetric in the two counterpropagating directions, strong competition is normally expected between the clockwise (CW) and counterclockwise (CCW) waves circulating in the ring cavity. As a result, ring diode lasers inherently exhibit directional switching and bistability behavior. In order to achieve unidirectional operation in ring diode lasers, it is necessary to introduce some asymmetric mechanisms into the ring cavity, such as spiral outcouplers [5] or S-section waveguides [3, 4].

With the TEC set near room temperature (15 °C), the dc laser operation of the ring diode lasers is observed at the ring pumping current of ~ 220 mA ($j_{th} \approx 713$ A/cm² at the ridge top). Fig. 4 shows the influence of the S-section bias on unidirectionality of ring diode laser R2, configured to favor the CW waves (*cf.* Fig. 2). Simultaneously collected signals from the integrated photodetectors PD1 (CW wave) and PD2 (CCW wave) are shown on a logarithmic scale by closed

and open symbols, respectively. When the S-section is left unbiased (or reverse-biased), a typical behavior is bidirectional lasing just above threshold (up to 10-20% above the threshold current) and lasing with predominance of one direction at higher currents. When the S-section is forward biased, significant improvement in unidirectionality of the lasing is observed. As shown in Fig. 4, the highest unidirectionality with counterpropagating wave suppression ratio exceeding 1000 (30 dB), or 99.99% power in the favorable CW direction, is obtained when the ring laser is pumped above 940 mA ($\sim 4.2 I_{th}$) and the S-section current is kept at 80 mA. This level of unidirectionality in QD ring lasers is much higher than in otherwise similar ring diode lasers with QW active regions [6].

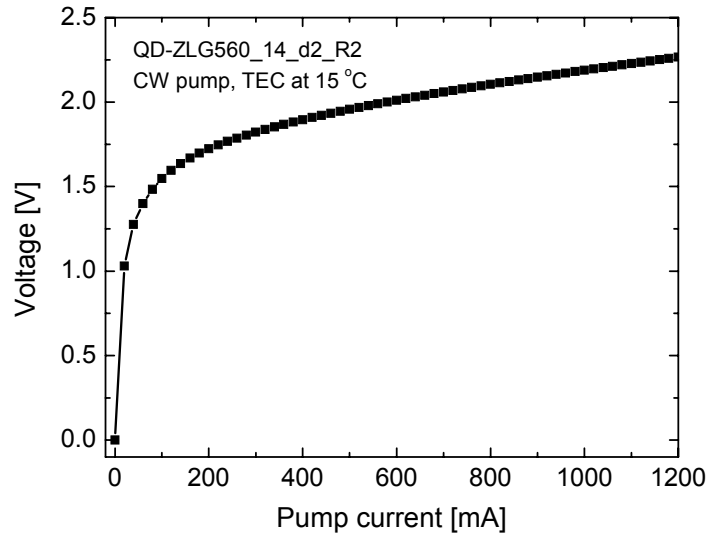


Fig. 3. The I - V curve measured on QD ring diode laser R2, indicating a normal p - n junction characteristic.

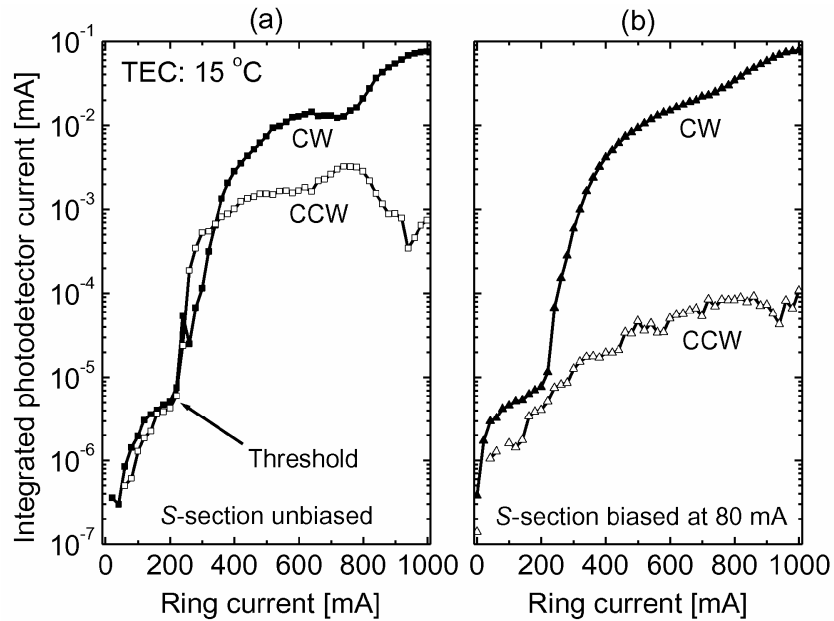


Fig. 4. L - I curves with photodetector signals shown in logarithmic scale. (a) When the S-section is unbiased, lasing operation occurs in both CW and CCW directions at nearly the same threshold current. (b) Pumping the S-section at 80 mA leads to a complete suppression of CCW lasing.

4. MICROWAVE MODE BEATING SPECTRA FROM INTEGRATED RING DIODE LASERS

4.1 Experimental setup

Detection of frequency-beating signals from monolithically integrated ring diode lasers is the basis of applications in gyro signal sensing, optical heterodyning, and high-speed signal generation. The output from individual lasers emitted in the desirable directions (as favored by the S-sections, see Fig. 2) is evanescently coupled out and directed to the mixer section, and then split between an integrated photodetector and a waveguide branched at the Brewster angle for external collection. The experimental setup for mode-beating measurement is schematically shown in Fig. 5. A beam splitter divides the external output into two parts. One part is sent to an optical spectrum analyzer (OSA). The other part is coupled to a high-speed photodetector; from which the signal is amplified and sent to an RF spectrum analyzer with bandwidth of 26 GHz.

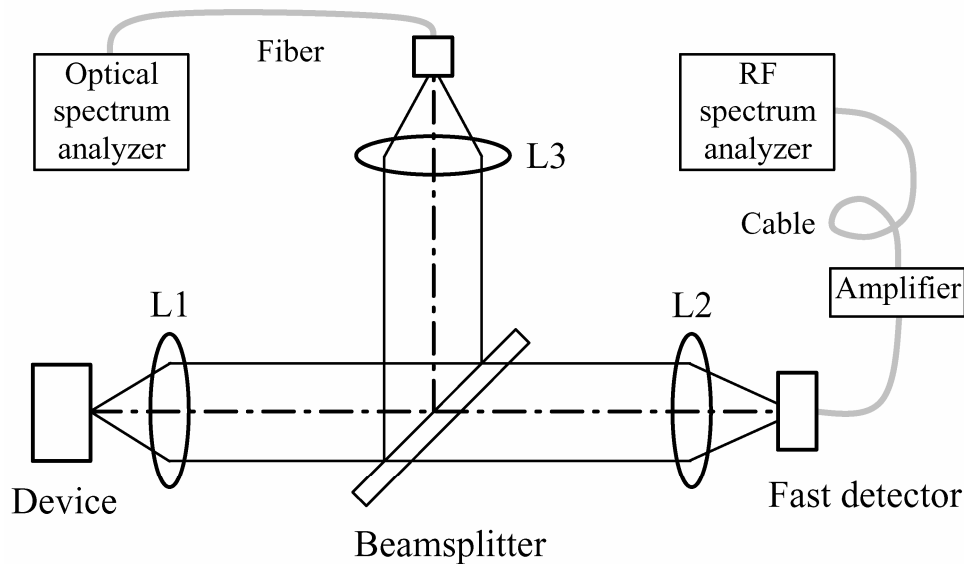


Fig. 5. Experimental setup for detection of beating signals from ring diode lasers. A beam splitter divides the optical output from the device, with one part sent to an optical spectrum analyzer and the other part coupled to a high-speed photodetector and an amplifier before it is sent to an RF spectrum analyzer with bandwidth of 26 GHz.

4.2 Mode beating spectra from individual ring lasers

The ring laser cavity is 10.28 mm in perimeter, with the corresponding longitudinal mode spacing frequency f of ~ 8.3 GHz. The laser operates in multiple longitudinal modes and its spectrum is centered at the wavelength of ~ 1250 nm. The waveguide WG-C, when kept unpumped, is not sufficiently transparent to transmit the emission from the weakly coupled ring lasers. Therefore, a forward bias is applied in order to improve waveguide transmission and provide signal amplification. Light output from a single ring diode laser through WG-C is detected by an external high-speed photodiode, and the signal is amplified and sent to an RF spectrum analyzer (see Fig. 5). A typical full-scan survey spectrum of mode beating from the ring diode laser R2 is shown in Fig. 6. Three beating lines appear at ~ 7.5 GHz, ~ 16.6 GHz, and ~ 25.1 GHz, corresponding to single, double, and triple longitudinal mode spacing in the ring cavity. It should be noted that the lines appearing at ~ 16.6 GHz and ~ 25.1 GHz, which correspond to $2f$ and $3f$ in the ring cavity, are quite stable, while the base line f is sometimes difficult to observe. Also, the detected frequency at ~ 7.5 GHz is not in exact multiple relation with other bands, which indicates some complicated lasing spectrum structure, with possible frequency shifts caused by nonlinear mode interactions [7]. The frequencies at $2f$ and $3f$ imply the group index of ~ 3.5 , in agreement with the index determined from spectral measurements on ridge-waveguide edge-emitting lasers fabricated from the same wafer.

To study the beating bands individually, different pumping conditions are applied to generate stable beating signals, and the signals are multiple-scan-averaged. Fig. 7 shows the resolved mode-beating spectra of multiple longitudinal modes of ring diode laser R2 at first, second, and third beating bands, respectively. The corresponding linewidths are 2.5 MHz, 4 MHz, and 10 MHz, respectively, indicating an increasing linewidth with higher mode-beating order.

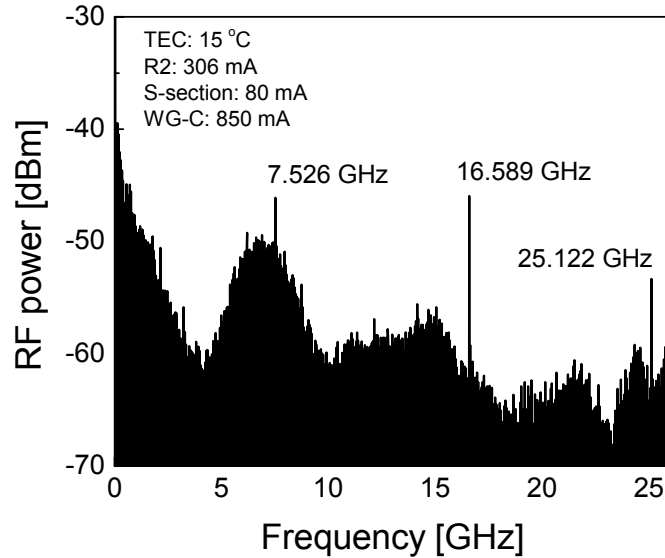


Fig. 6. A survey spectrum of mode beating from the ring diode laser R2. Three beating lines appear at ~ 7.5 GHz, ~ 16.6 GHz, and ~ 25.1 GHz, corresponding to single, double, and triple longitudinal mode spacing in the ring cavity.

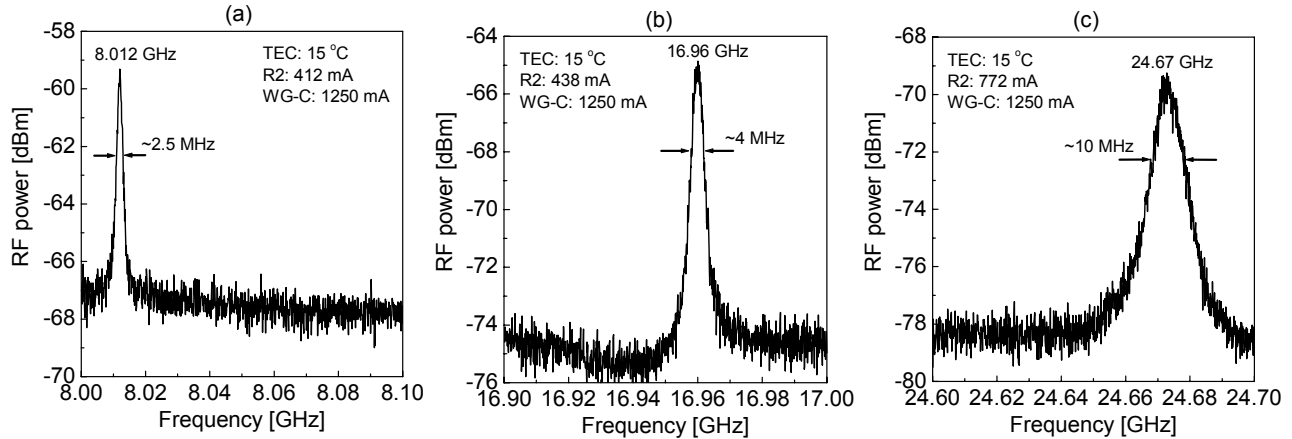


Fig. 7. Resolved mode-beating spectra (multiple-scan-averaged) of multiple longitudinal modes of the ring diode laser R2 in first (a), second (b), and third (c) beating bands. Note that the linewidth increases with higher mode-beating order.

4.3 Mode beating spectra from integrated twin ring diode lasers

The arrangement of the experimental setup as shown in Fig. 5 enables the detection of both optical spectra and RF beating spectra at the same time, which is especially useful in measurements of beat note between twin ring diode lasers. Normally, the frequency difference between the two beams from R1 and R2 is much bigger than 26 GHz. For this reason, the OSA is used to monitor the optical spectra during the coarse tuning by adjusting the currents driving the

two lasers. In our earlier measurements with QW-based ring diode lasers, both rough tuning by pumping current and fine tuning by integrated Joule heaters have been demonstrated [5]. Similarly, in the present case of the QD-based devices, it is possible to roughly overlap the output spectra from twin ring lasers by adjusting the pumping currents on ring lasers R1 and R2 (and thereby controlling the optical spectrum in the wavelength range of 1240-1260 nm). Fig. 8 shows a typical line of mode beating between the twin ring diode lasers at ~ 12.3 GHz, with the linewidth of ~ 4 MHz. By changing the pump currents on both rings, another beat note appears at ~ 2.9 GHz. Fig. 9(a) shows this signal with resolved structure and the linewidth of ~ 44 MHz, increased due to multiple-scan-average. The corresponding optical spectrum measured by OSA is shown in Fig. 9(b), indicating a complex multimode structure. Studies of spectral tuning by pumping currents and by separate Joule heaters are still in progress.

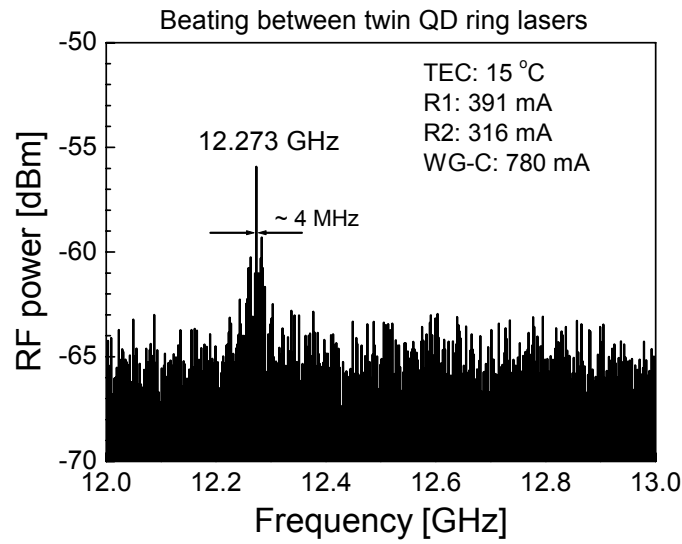


Fig. 8. A typical line of mode beating between integrated twin ring diode lasers R1 and R2 at ~ 12.3 GHz, with the linewidth of ~ 4 MHz.

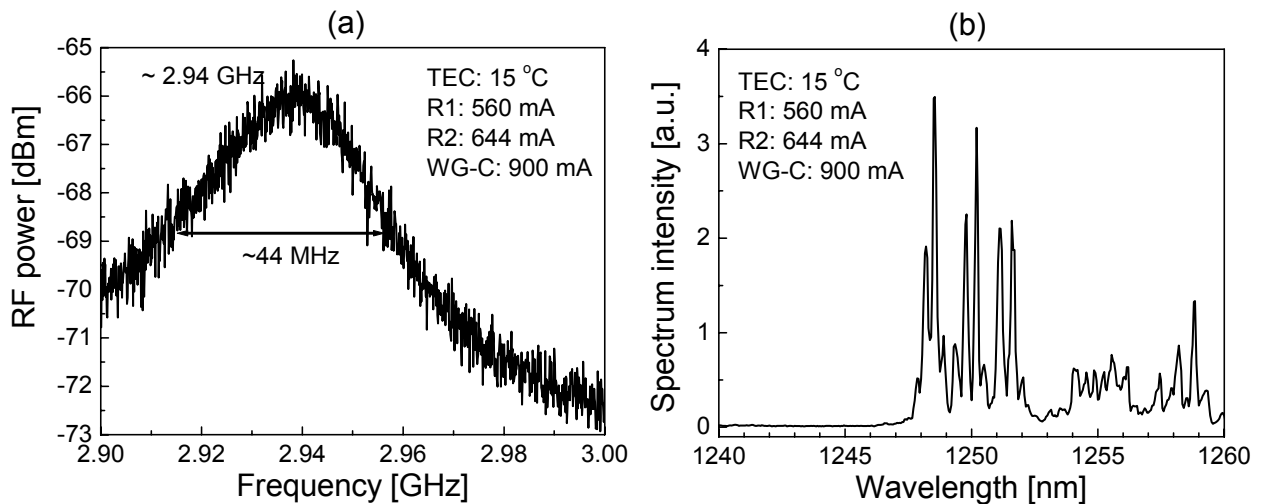


Fig. 9. (a) Resolved mode-beating spectrum (multiple-scan-averaged) between integrated twin ring diode lasers R1 and R2 at ~ 2.9 GHz, with the linewidth of ~ 44 MHz. (b) The corresponding optical spectrum indicates a complex multimode structure.

5. DISCUSSION

The mechanism of directional competition and control in S-section SRLs is rather complicated, as it can be influenced by multiple phenomena, such as conservative and dissipative scattering [8], nonlinear saturation effects, and multi-longitudinal-mode interactions, in addition to redirection of light through the S-section. Our results indicate that the spontaneous emission seeding also plays an important role in directional competition. When the S-section is unbiased or reverse-biased, directional control relies mainly on loss difference between the CW and CCW waves. In the configuration of R2 as shown in Fig. 2, this selection mechanism is not sufficient to assure operation in the favored direction, as the coupling of CCW light from the ring into the S-section is relatively small. In contrast, spontaneously emitted light from the S-section is strongly coupled to the ring, which explains why the forward biasing of the S-section is very effective in maintaining stable unidirectional operation in the favored direction.

Other factors that likely contribute to higher CWSR in QD-based ring lasers include low threshold current density and low internal loss [2] (implying low backscattering), as well as a lower density of states that results in earlier saturation of absorption in the unbiased S-section. Determination of relative contributions of various mechanisms of counterpropagating mode competition in ring diode lasers requires further studies.

Beating signals are produced by pairs of oscillating modes in the laser emission. It is obvious that in both single and twin ring diode laser cases the optical spectra are multimode. Each beating line can be produced by a number of pairs. There are many longitudinal modes excited with almost fixed mode spacing. From a single pair of modes, the beating linewidth is determined by convolution of individual optical linewidths. When many pairs give overlapping lines, additional broadening appears. The mode spacing is not perfectly constant due to dispersion of the group index. This dispersion is sensitive to laser design and can be very low in low-dimensional laser structures. In general, the dispersion should be accounted as a factor that can contribute to spectral broadening of observed beating lines.

The lines of beating between two ring lasers are also produced by sets of longitudinal modes. In this case, an additional broadening can be associated with non-equivalence of ring lasers. The design and fabrication technologies provide accurately the same cavity size. However, the detuning of lasers is associated with local temperature variations, wafer nonuniformities, etc., therefore some deviation from equivalence can be expected.

Beating in the twin ring laser system can be inspected for frequency lock-in effect that is known as an obstacle in the gyroscopic application of ring lasers. This effect produces a dead range of beating frequencies, where the frequency is equal to zero due to pulling of optical frequencies to each other. The dead range is sensitive to backscattering and other coupling mechanism between modes. In a twin ring system these coupling factors are minimized as the mode volumes of particular modes in each pair are not overlapping at all. However, the linewidth of the observed beating line provides the upper limit for the dead range.

Compared to QW-based twin ring diode lasers reported earlier [5], we notice several features of the QD-based structures: 1) beating signals from longitudinal modes are narrower, although weaker in intensity; 2) group index of the laser medium is lower (3.5 against 3.85 in QWs); 3) the envelope optical spectrum is wider; 4) no power-dependent splitting of longitudinal-mode beating line [7] is observed. We associate these properties with the following physical features of the QD structures: large contribution of inhomogeneous broadening in the gain band, smaller linewidth broadening factor, and lower optical power per oscillation mode.

6. CONCLUSIONS

In conclusion, we report on fabrication and characterization of optoelectronic integrated circuits incorporating optically independent twin ring diode lasers with InAs/InGaAs/GaAs DWELL active region. Directional control is demonstrated by forward biasing the S-section, with stable traveling-wave (unidirectional) operation characterized by the suppression ratio of counterpropagating waves as high as 30 dB. Longitudinal-mode-beating spectra are observed in the frequency range up to 26 GHz; peaks corresponding to difference frequency of single, double, and triple orders are measured.

Mode beating spectra between integrated twin ring diode lasers are reported at both ~ 2.9 GHz and ~ 12.3 GHz, with minimal linewidth of ~ 4 MHz.

ACKNOWLEDGMENTS

This work was supported by the National Science Foundation (NSF Grant ECS-0524509). The authors acknowledge fruitful discussions with Dr. Petr G. Eliseev at the Center for High Technology Materials, University of New Mexico.

REFERENCES

1. E. J. Post, "Sagnac effect", *Rev. Mod. Phys.* **39**, pp. 475-493 (1967).
2. G. T. Liu, A. Stintz, H. Li, K. J. Malloy, and L. F. Lester, "Extremely low room-temperature threshold current density diode lasers using InAs dots in $\text{In}_{0.15}\text{Ga}_{0.85}\text{As}$ quantum well", *Electron. Lett.* **35**, pp. 1163-1165 (1999).
3. J. P. Hohimer, G. A. Vawter, and D. C. Craft, "Unidirectional operation in a semiconductor ring diode laser", *Appl. Phys. Lett.* **62**, pp. 1185-1187 (1993).
4. H.-J. Cao, H. Deng, H. Ling, C.-Y. Liu, V. A. Smagley, R. B. Caldwell, G. A. Smolyakov, A. L. Gray, L. F. Lester, P. G. Eliseev, and M. Osiński, "Highly unidirectional InAs/InGaAs/GaAs quantum-dot ring lasers", *Appl. Phys. Lett.* **86**, Art. 203117 (2005).
5. H.-J. Cao, C.-Y. Liu, H. Ling, H. Deng, M. Benavidez, V. A. Smagley, R. B. Caldwell, G. M. Peake, G. A. Smolyakov, P. G. Eliseev, and M. Osiński, "Frequency beating between monolithically integrated semiconductor ring lasers", *Appl. Phys. Lett.* **86**, Art. 041101 (2005).
6. H.-J. Cao, H. Ling, C.-Y. Liu, H. Deng, M. Benavidez, V. A. Smagley, R. B. Caldwell, G. M. Peake, G. A. Smolyakov, P. G. Eliseev, and M. Osiński, "Large S-section-ring-cavity diode lasers: directional switching, electrical diagnostics, and mode beating spectra", *IEEE Photon. Technol. Lett.* **17**, pp. 282-284 (2005).
7. C. Liu, H. Cao, G. A. Smolyakov, P. G. Eliseev, and M. Osiński, "Anomalous splitting in microwave mode-beating spectra of semiconductor ring lasers", *Electron. Lett.* **41**, pp. 963-964 (2005).
8. M. Sorel, G. Giuliani, A. Scire, R. Miglierina, S. Donati, and P. J. R. Laybourn, "Operating regimes of GaAs-AlGaAs semiconductor ring lasers: Experiment and model", *IEEE J. Quantum Electron.* **39**, pp. 1187-1195 (2003).